IEEE Access
Multidisciplinary | Rapid Review | Open Access Journal

Date of publication xxxx 00, 0000, date of current version xxxx 00, 0000.

*Digital Object Identifier 00.0000/ACCESS.2019.DOI*

# Robustness-Driven Hybrid Descriptor for Noise-Deterrent Texture Classification

**AYESHA SAEED[1], FAWAD[1], (Student Member, IEEE), MUHAMMAD JAMIL KHAN[1], (MEMBER, IEEE), MUHAMMAD ALI RIAZ[1], (MEMBER, IEEE), HUMAYUN SHAHID[1],(MEMBER, IEEE), MANSOOR SHAUKAT KHAN[2], YASAR AMIN[1], (SENIOR MEMBER, IEEE), JONATHAN LOO[3], (MEMBER, IEEE), AND HANNU TENHUNEN[4,5], (MEMBER, IEEE)**

[1]ACTSENA Research Group, Telecommunication Engineering Department, University of Engineering and Technology Taxila, Punjab, 47050, Pakistan
[2]Mathematics Department, COMSATS University Islamabad, Park Road, Tarlai Kalan, Islamabad 45550, Pakistan
[3]School of Computing and Engineering, University of West London, St Mary's Road, Ealing, W5 5RF, London, United Kingdom
[4]Department of Electronic Systems, Royal Institute of Technology (KTH), Isafjordsgatan 26, Stockholm, SE 16440, Sweden
[5]Department of Information Technology, TUCS, University of Turku, Turku 20520, Finland

Corresponding author: Fawad (e-mail: engr.fawad@students.uettaxila.edu.pk).

The work was supported by Higher Education Commission (HEC) of Pakistan under Technology Development Fund TDF-67/2017 and ASR&TD-UETT faculty research grant.

**ABSTRACT** A Robustness-Driven Hybrid Descriptor (RDHD) for Noise-deterrent Texture classification is presented in this paper. This work offers the ability to categorize a variety of textures under challenging image acquisition conditions. An image is initially resolved into its low-frequency components by applying wavelet decomposition. The resulting low-frequency components are further processed for feature extraction using completed joint-scale local binary patterns (CJLBP). Moreover, a second feature set is obtained by computing the low order derivatives of the original sample. The evaluated feature sets are integrated to get a final feature vector representation. The texture-discriminating performance of the hybrid descriptor is analyzed using renowned datasets: Outex original, Outex extended and KTH-TIPS. Experimental results demonstrate a stable and robust performance of the descriptor under a variety of noisy conditions. An accuracy of 95.86%, 32.52% and 88.74% at noise variance of 0.025 is achieved for the given datasets, respectively. A comparison between performance parameters of the proposed work with its parent descriptors and recently published work is also presented.

**INDEX TERMS** Feature descriptor, Texture classification, Gaussian derivatives, Wavelet decomposition, Local binary pattern, Noise robust

## I. INTRODUCTION

In image processing, the texture is a measure of the visual appearance of an object such as smoothness, roughness, and grainy nature, etc., It is a fundamental feature of natural images and represents the complexity of the spatial arrangement of local pixels. A plethora of texture categories exist in nature. Texture classification is the process of categorization based on its unique characteristics [1] [2]. Applications of texture classification include: detection of surface defects [3] [4], identification of tissues in tomography images [5] [6] [7], robotic vision [8] [9] [10] [11] [12], analysis of sonar imagery [13], recognition of facial expressions [14] [15], detection of a moving object [16] [17]. The performance of texture classification depends on two main factors: 1) image feature representation and (2) feature classification. A feature vector must uniquely be able to distinguish an image. If the features are not unique to the texture, accurate classification performance cannot be achieved [1]. The properties for a desirable feature vector are as follows: The features should be (1) discriminating [18] [19] [20] [21], (2) noise robust [8] [9], (3) invariant to image orientation and lighting changes [2] [22] [23], (4) smaller in dimension [24] [25], and (5) efficient in implementation [26] [39]. The proposed work mainly focuses on the performance of texture classification in the presence of noise. Noise is the random change in the image pixel intensities that can occur either during image acquisition or in the transmission link [27]. This random variation affects the feature representation of the image and thus results in inaccurate classification [28] [29]. In recent literature, numerous methods for noise-robust categorization

This article has been accepted for publication in a future issue of this journal, but has not been fully edited. Content may change prior to final publication. Citation information: DOI 10.1109/ACCESS.2019.2932687, IEEE Access



of texture have been proposed.

This work proposes a method for robust classification of texture by transforming an image into a noiseless representation. This is accomplished by using a wavelet transform that effectively represents an image into its low-frequency components. The presented framework is divided into the following steps: Initially, an image is resolved into its low noise coefficients using a wavelet transform and LBP based textural features are extracted. Afterward, the first and second order differential responses of the original sample are calculated and transformed into a feature representation. The two feature sets are integrated to form a final feature representation. Experimental results prove the continuous high discriminating and robust performance in the presence of Additive White Gaussian Noise. The proposed RDHD provide more deterrence against additive white Gaussian noise, as well as invariance to orientation, scale, and illumination changes when evaluated on Outex, Outex extended [53], and KTH-TIPS [54] dataset on several recently reported descriptors.

Remaining contents of the paper are organized as follows. Sect. II reviews methodology of important related texture descriptors, Sect. III discusses proposed hybrid descriptor, Sect. IV details the experimental setup (noise conditions, datasets and classification algorithm), Sect. V covers the analysis of noise robustness and discusses the results of the proposed descriptor while Sect. VI concludes the paper.

## II. RELATED WORK

We start our discussion from a popular feature descriptor, Local Binary Pattern (LBP), proposed by Ojala et al. [30]. The texture operator fulfills the characteristics necessary for an ideal feature descriptor, except that it is noise intolerant [46]. LBP considers a small circular area of pixels in an image and computes pixel differences against the center pixel value. The differences are then converted to binary representation using a threshold function. The problem arises when noise corrupts the center pixel value in the smooth gray intensity region; thus the texture pattern is changed [35] [49]. The issue of noise intolerance associated with LBP is solved by another operator LTP (Local Ternary Pattern) [31]. The authors propose to introduce a user-defined threshold that changes the central pixel value. This, in turn, allows preserving the original textural pattern in the smooth gray intensity region. Some other methods that add noise robustness to the LBP texture representation are as follows. Soft LBP (SLBP) has been proposed by Ahonen et al. [32]. The operator achieves noise robustness by replacing the threshold dependent function in LBP with a fuzzy logic function. Another method, Noise Resistant LBP (NRLBP) is proposed in [33], which recovers the noise-free LBP pattern from a noisy pattern by assigning a random state to the minute pixel differences in the smooth region and then sets a value such that a noise-free coded pattern is formed. If no noise free pattern can be formed, then a noisy non-uniform pattern is maintained. Chen et al. have proposed Robust LBP (RLBP) [34]. It translates the noisy codes to noise-free uniform codes by changing the specified bit of LBP. The results show that RLBP is more noise robust than LBP.

In [41] Haar wavelet, Ridgelet, and Fourier transform applied to the input image before the feature extraction process. This approach provides rotation invariance for the noisy texture, but in the presence of scale, and illumination variations its performance degrades. In [42], the rotation and scale invariant texture representation is obtained through Local Gabor Wavelets Binary Patterns (LGWBPs). However, LGWBPs contain redundant features, which increases the time complexity as well as degrade the efficiency. In [43] Extended Mapping Local Binary Pattern (EMLBP) is proposed, which provides the rotation invariant version of the local binary pattern. However, the descriptor is very sensitive to the noise in the input images. The Overlapped Multi-oriented Tri-scale Local Binary Pattern (OMTLBP) [44] is robust against AWGN noise even in the presence of variations in orientation, scale, and illumination. However, the feature vector of OMTLBP is large.

A completed representation of LBP (CLBP) is proposed by Guo et al. [45]. In contrast to LBP, which considers only the signs of differences for the feature representation, CLBP considers the sign along with the magnitude of differences as well as the center gray value of the local circular region. The features corresponding to the sign, magnitude, and center components are integrated to obtain an improved texture characterization. The magnitude and center components are based on global mean thresholding operation, which provides noise robustness. Song et al. [36] have computed local contrast patterns (LCPs) from their own designed set of difference kernels. After application of kernels, the LCPs are obtained by converting the resulting responses into their coded versions. A final texture feature representation is obtained by combining LCPs from each kernel. LCP outperforms LBP, LTP, and CLBP in the presence of noise. In MRELBP [39], Liu et al employ local image medians of pixels rather than local pixel brightness to achieve a noise robust feature representation.

BRINT (Binary Rotation Invariant and Noise Tolerant) texture operator is proposed by Liu et al. [35]. BRINT is established on the rotation invariant version of LBP. In contrast to LBP, BRINT can represent a circular pixel area of any size. It produces permanent dimensionality feature histogram irrespective of the scale chosen. BRINT takes an average of the pixels along a circular arc for a given scale of the region. The approach keeps the number of pixels in the local patch fixed at eight. Pan et al. proposed a highly robust and low dimensional descriptor, DLABP (Diamond Local Adaptive Binary Pattern) [40]. It employs a diamond-shaped local neighbor structure. A fixed number of eight neighbor pixels in the diamond-shaped local patch provides a discriminative and low dimensional feature vector. In con-

This article has been accepted for publication in a future issue of this journal, but has not been fully edited. Content may change prior to final publication. Citation information: DOI 10.1109/ACCESS.2019.2932687, IEEE Access



trast to BRINT, averaging is done in the radial direction along multiple scales. DALBP shows performance close to BRINT while it surpasses LBP, LTP, CLBP and MRELBP. Averaging operation on pixels results in a low frequency extraction of texture information and thus making the pattern more robust to noise. Joint of scales Local Binary Pattern, JLBP [46] goes one step ahead of the approaches devised in BRINT and DALBP. JLBP performs pixel averaging first on the same scale and then on multiple scales, starting from the largest scale. Therefore, JLBP achieves better noise robustness. In [48], a noise robust texture descriptor LETRIST (Locally Encoded Transform Feature Histogram) is presented. In LETRIST noise robustness is achieved using low order filters and global mean for preparation of texture codes.

## III. PROPOSED HYBRID DESCRIPTOR

This section outlines the steps to formulate a discriminating and noise-deterrent representation of image texture. The proposed framework is a combination of two feature sets. The first feature set is extracted from wavelet approximated sub-image, while the second feature set is obtained through the Gaussian derivative filter response. The DWT provides shift invariance and noise robustness to the first feature set of our proposed method [50]. The CJLBP descriptor contains a multi-scale fusion stage, which offers scale invariance to the proposed framework. The multi-scale fusion stage of CJLBP is modified to enhance the scale invariance of the descriptor as shown in Fig. 1. Equal weight is assigned to each element of the fused patch in the modified CJLBP. Using a feature set based on Gaussian derivative filters enhances the discriminative power of the proposed hybrid texture descriptor. Fig. 1 provides a road-map for the proposed scheme composed of three sequential stages detailed as follows.

### A. MULTI-RESOLUTION DECOMPOSITION

Conversion of the input image data into low-frequency components serve as the first step towards setting up a discriminant and noise-robust texture representation. The proposed descriptor requires to transform the input image into a noise-free representation while retaining spatial information. The above is achieved using multi-resolution analysis wherein efficient representation of the input image in the spatial-frequency joint domain allows for spectral components to be analyzed locally. 2D discrete wavelet transform is used to decompose the input image into its constituent low-frequency components via discrete approximation of Meyer (commonly referred to as demey waveform) [51] [52]. The wavelet transformation of the input image results in four sub-bands: one approximate and three detailed images. The proposed descriptor focuses on low-frequency, noise-free components present in the approximated sub-image, and largely ignores the information content in the detailed sub-images. The approximate sub-image contains the low-frequency (noiseless) information from the whole image. The decomposition of a noisy image into its sub-images is represented in Fig. 2 (a). Let $N(p_x, p_y)$ represent a noisy image of size $P_x \times P_y$, where $p_x$ and $p_y$ are the positions of pixel intensities in horizontal and vertical directions, respectively. Now, let $W(w_x)$ represent a 1-D low pass filter of size $w_x$ applied horizontally along the image $N(p_x, p_y)$. The resulting image $N_L(p_{x1}, p_y)$ is represented in (1).

$$N_L(p_{x1}, p_y) = S\big(N(p_x, p_y) * W(w_x)\big). \tag{1}$$

where $S(.)$ is a desampling operator applied along x-direction and $p_{x1} = p_x/2$. Similarly, we apply $W(w_y)$ vertically on $N_L$. The image $N_{LL}(p_{x1}, p_{y1})$ is represented in (2) and is one fourth of size of $N(p_x, p_y)$.

$$N_{LL}(p_{x1}, p_{y1}) = S\big(N_L * W(w_y)\big). \tag{2}$$

where, $*$ denotes convolution operation and $p_{y1} = p_y/2$. $N_{LL}(p_{x1}, p_{y1})$ represents the approximated sub-image and is utilized for feature extraction as discussed in the next step.

### B. FEATURE COMPUTATION

Feature computation plays a very critical role in the proposed framework as: 1) the choice of feature descriptors affects the discrimination power of the proposed hybrid descriptor. 2) feature extraction from low-frequency data does not apply to all kinds of feature descriptors. Therefore, we aim to compute features that are noise potent and discriminative at the same time. We start our discussion from the computation of robust noise features. The first set of features is based on LBP descriptor. The LBP operator does not involve the calculation of higher order statistics (such as $2^{nd}$ order pixel-differences); therefore the extraction of features from the low noise data improves the performance of the hybrid descriptor. Among the LBP based descriptors, we use CJLBP operator for feature portrayal. We choose CJLBP_SMC operator of the CJLBP descriptor. We have modified the multi-scale fusion stage of CJLBP to improve the scale invariance of the descriptor as shown in Fig. 2(b). Equal weight is assigned to each element of the fused patch in the modified CJLBP. The low-frequency sub-band $N_{LL}$ as shown in (2) is used for feature extraction. Since the features are obtained from the wavelet approximation of the image, the obtained feature vector is notated as WCJ_SMC since the features are obtained from the wavelet approximation of the image.

$$\begin{aligned} &WCJ\_SMC = \\ &= X(WCJ\_S, WCJ\_M, WCJ\_C). \end{aligned} \tag{3}$$

where X(.) presents the combination of the three individual operators WCJ_S, WCJ_M, and WCJ_C into a final operator WCJ_SMC shown in Fig. 1 (c). WCJ_S is extracted from the approximated image in a similar way as described in CJLBP_S [46]. The magnitude and center operators for two scales Y = (y1, y2) and sample points T are presented as follows.

This article has been accepted for publication in a future issue of this journal, but has not been fully edited. Content may change prior to final publication. Citation information: DOI 10.1109/ACCESS.2019.2932687, IEEE Access



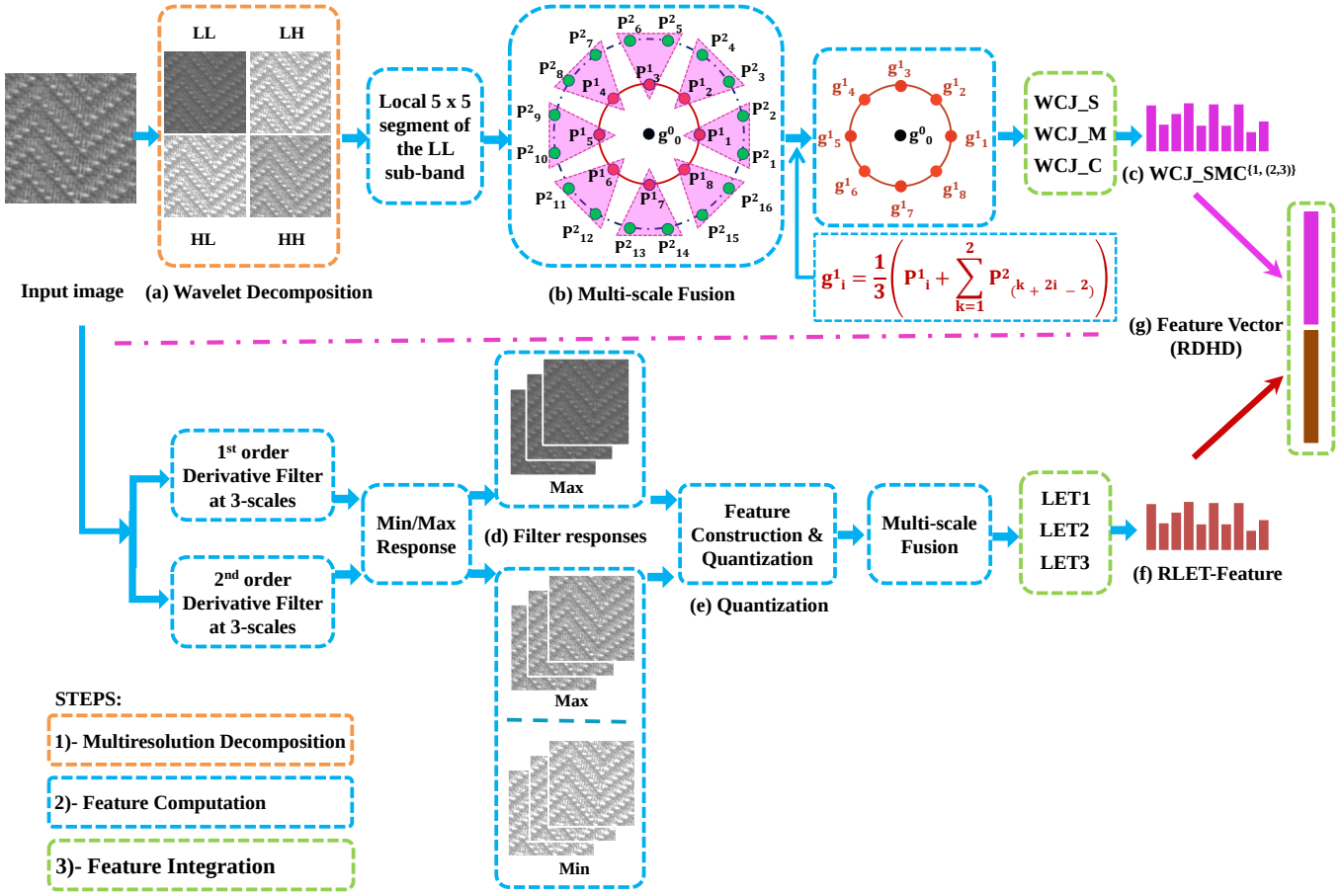


**FIGURE1:** The flow diagram of our proposed Robustness-Driven Hybrid Descriptor (RDHD) for texture representation.

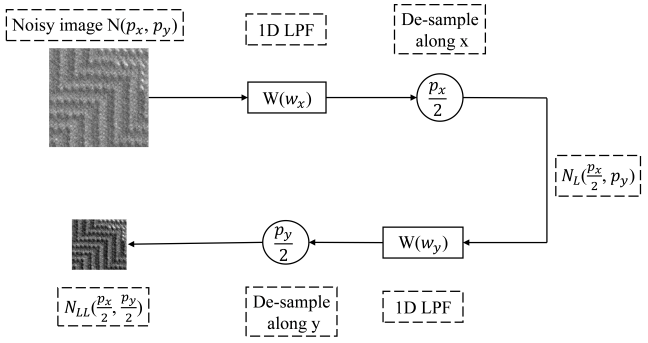


**FIGURE2:** Wavelet decomposition using subband coding.

$$WCJ\_M_{T,y1,y2} = \\ = \sum_{t=0}^{T-1} s(m_{t,y1} + m_{t,y2} - c_{y1} - c_{y2})2^t. \quad (4)$$

where $m_{t,y_n}$ is the absolute difference of the $t^{th}$ neighborhood of center pixel in the local segment at scale $y_n$. The $c_{y_n}$ is the average value of $m_{t,y_n}$ of whole image. The center component is represented as:

$$WCJ\_C_{T,Y} = s(2g_{c,y1,y2} - c). \quad (5)$$

$$s(x) = \begin{cases} 1 & x \geq 0 \\ 0 & x < 0. \end{cases} \quad (6)$$

where $g_c$ is the central pixel of the local segment, $c$ represents mean gray intensity of the whole image and $s$ is binary threshold operator and is defined in (6). The choice of parameters is discussed as follows. The operator uses a fixed number of local neighbors, T = 8 and a joint of scales Y = (3, 2) is used to compute classification performance.

After the computation of robust noise features, we now calculate a second feature set that improves the discrimination power of the hybrid descriptor. We choose the quantized max/min filter response to calculate the second feature set. This computes texture based on first and second order Gaussian derivative filters as shown in Fig. 1 (d). The choice of the second feature set contributes diverse features to our proposed feature vector. The initial feature vector consists of variables that are based on first order pixel differences.

This article has been accepted for publication in a future issue of this journal, but has not been fully edited. Content may change prior to final publication. Citation information: DOI 10.1109/ACCESS.2019.2932687, IEEE Access



This implies that the addition of second-order derivative features will add discrimination to our proposed feature representation. The second feature set is directly extracted from the noisy image $N$, as it requires to compute both low and high-frequency image statistics, for example, first and second order derivative responses, respectively. Therefore, it is best to use the initial image (without wavelet dissection). The feature vector is computed as followed by LETRIST operator. Firstly, the low order Gaussian derivative filters are applied to the noisy image $N$, and the extrema responses are calculated. This is represented mathematically as follows.

$$N^{\theta}_{1max} = \sqrt{N_1^{x^2} + N_2^{y^2}}. \tag{7}$$

$$N^{\theta}_{2max} = \frac{1}{2}\left(N_2^x + N_2^y + \sqrt{(N_2^x - N_2^y)^2 + 4N_2^{xy^2}}\right). \tag{8}$$

$$N^{\theta}_{2min} = \frac{1}{2}\left(N_2^x + N_2^y - \sqrt{(N_2^x - N_2^y)^2 + 4N_2^{xy^2}}\right). \tag{9}$$

$$H_1^{\theta} = \cos(\theta)H_1^x + \sin(\theta)H_1^y. \tag{10}$$

and

$$H_2^{\theta} = \cos^2(\theta)H_2^x + \sin^2(\theta)H_2^y - \sin(2\theta)H_2^{xy}. \tag{11}$$

where $N_1^{\theta} = N_1 * H_1^{\theta}$ and $N_2^{\theta} = N_2 * H_1^{\theta}$, the first and second order filters $H_1^{\theta}$ and $H_2^{\theta}$ are described mathematically in (10) and (11) and $*$ denotes the convolution operation. The $H_n$ is the Gaussian $n^{th}$ order derivative filter at the rotation angle $\theta$ and $H_1^x$, $H_1^y$, $H_2^x$, $H_2^y$ are the x and y first and second order derivatives respectively, and $cos\theta$, $sin\theta$ are the interpolation parameters for the basis functions [48]. The extrema responses are computed at three scales e.g., $N_{\sigma^2} = 3$. Now the transformed features $T = \{G, D, S, R\}$ are computed using the extrema responses as follows.

$$G = N^{\theta}_{1max} = \sqrt{N_1^{x^2} + N_1^{y^2}}. \tag{12}$$

$$D = N^{\theta}_{2max} - N^{\theta}_{2min} = \sqrt{(N_2^x + N_2^y)^2 + 4N_2^{xy^2}}. \tag{13}$$

and

$$\begin{aligned} S &= \frac{1}{2} - \frac{1}{\pi}\tan^{-1}\frac{-N^{\theta}_{2max} - N^{\theta}_{2min}}{(N^{\theta}_{2max} - N^{\theta}_{2min})}. \\ &= \frac{1}{2} - \frac{1}{\pi}\tan^{-1}\frac{-N_2^x - N_2^y}{\sqrt{(N_2^x - N_2^y)^2 + 4N_2^{xy}}}. \end{aligned} \tag{14}$$

$$\begin{aligned} R &= \frac{2}{\pi}\tan^{-1}\frac{N^{\theta}_{2max} - N^{\theta}_{2min}}{(N^{\theta}_{1max}} \\ &= \frac{2}{\pi}\tan^{-1}\left(sc \times \frac{D}{G}\right). \end{aligned} \tag{15}$$

where $sc$ is a parameter to control the value of $R$. Now the transformed features $\{G, D\}$ and $\{S, R\}$ are converted to binary codes by using the quantizers $B_1(x)$ and $B_2(x)$ as shown in (16) and (17), respectively.

$$B_1(x) = \begin{cases} 0 & \frac{X}{m_X} > p \\ 1 & otherwise \end{cases} \tag{16}$$

$$B_2(x) = \begin{cases} 0 & X \in [0, \delta] \\ 1 & X \in [\delta, 2\delta] \\ \dots & \\ A-1 & X \in [(A-1)\delta, 1] \end{cases} \tag{17}$$

where, $X \in \{G, D\}$, $m_X$ and is the average of the transmute feature map of $x$ and $p$ is a scalar of control. The $X \in \{S, R\}$ and $A$ is the calibration level so the calibration step is $\delta = \frac{1}{L}$. For a discerning feature vector calibration level is set to $L_S = 3$ and $L_R = 5$ for $si$ and $r$ transmute features, respectively. The quantization levels are set to $L_S = 3$, $L_R = 5$ and $L_G = L_D = 2$. The Quantization stage is shown in Fig. 1 (e). The three histograms namely $LET1$, $LET2$ and $LET3$ are built using the combinations of $\{G, D, S\}$ across adjacent scales $(\sigma_1^2, \sigma_2^2)$ and $(\sigma_2^2, \sigma_3^2)$ and $\{R\}$ across the three scales, $(\sigma_1^2, \sigma_2^2, \sigma_3^2)$ respectively. The three histograms are concatenated to form Robust Locally Encoded Transformed (RLET) feature vector shown in Fig. 1 (f).

$$RLET = LET1 \| LET2 \| LET3. \tag{18}$$

where, $\|$ denotes the concatenation operation. RLET features contribute necessary discrimination power to the hybrid descriptor which is required at the high noise level.

### C. FEATURE INTEGRATION

After feature computation, we now join the two histogram based feature sets into a joint representation as shown in Fig. 1 (g). Let $f_1(.)$ and $f_2(.)$ represent the computation of two feature sets on the wavelet resolved image $N_{LL}$ and noisy image N, respectively. Then, the image statistics RDHD (Robustness-Driven Hybrid Descriptor) presents a discriminating and noise robust texture representation. This is expressed as follows.

$$RDHD = f_1(N_{LL}(p_{x1}, p_{y1})) \| f_2(N(p_x, p_y)). \tag{19}$$

where, $\|$ denotes the concatenation operation on the two sets of features.

The hybrid descriptor RDHD has a feature dimension that is the sum of the number of variables in individual feature vectors. The first feature set consists of a 200-bin histogram while the second feature set represents a 413-bin histogram. Thus, the final feature set represents a 613-bin histogram.

The proposed hybrid descriptor has the following properties. It is highly discriminative, invariant to image transformations, e.g., rotation, illumination, scale and pose variations, robust to noise, and efficient in implementation. In the

This article has been accepted for publication in a future issue of this journal, but has not been fully edited. Content may change prior to final publication. Citation information: DOI 10.1109/ACCESS.2019.2932687, IEEE Access



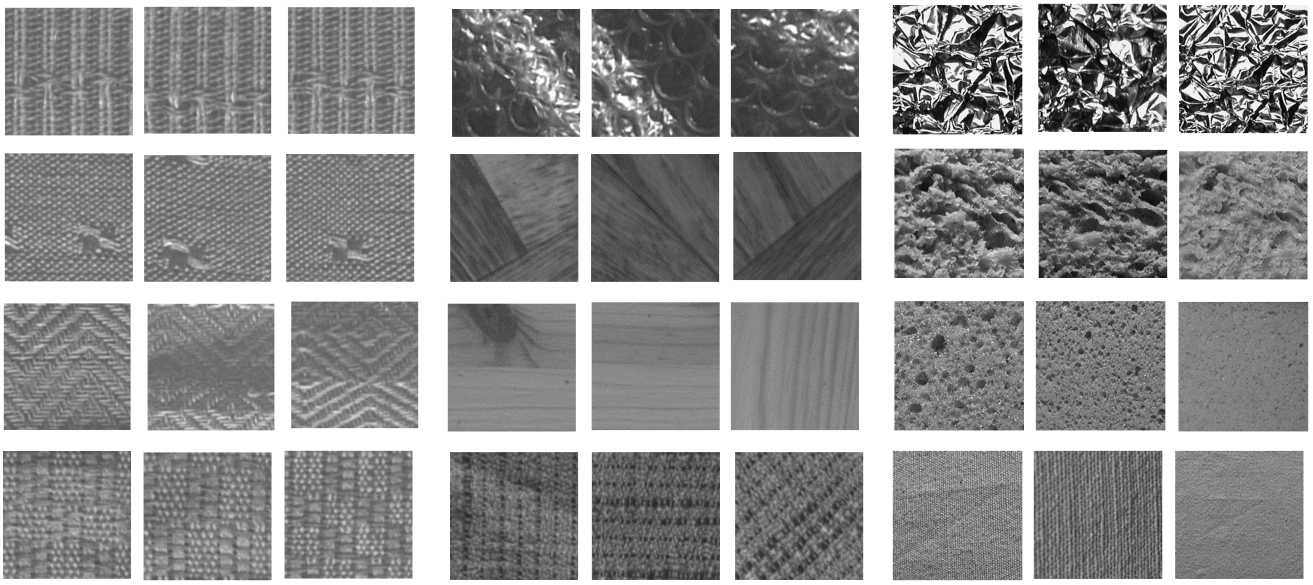


**FIGURE3:** Sample images from three datasets: (a) Outex Original, (b) Outex Extended and (c) KTH-TIPS. Four classes from each dataset are displayed along rows. Three samples from each class are displayed along columns.

results section, we validate the above arguments through the evaluation of classification performance on relevant datasets. The discrimination is provided by the computation of two contrasting feature sets. Robustness against the rotation of texture is provided from the encoding of an individualize texture pattern at multiple angles using the LBP's rotation invariance methodology and steerable Gaussian derivative filters. Robustness against gray scaling and shifting is provided through the use of difference operator while computing the two feature sets, which effectively cancels out the gray shift. The Gray scaling is avoided from the use of global gray-mean value in the quantization step.

## IV. EXPERIMENTAL SETUP

To demonstrate the discriminating and noise resistant property of our feature descriptor, we perform experimentation on three texture datasets, Outex Org. (original), Outex Ext. (extended) and KTH-TIPS. The example images of each dataset are displayed in Fig. 3. The datasets are modified in relevance to our work and images are deprived of additive white Gaussian noise (AWGN), with zero mean. For a comprehensive study, we divide the experimental setup into two parts. The first experiment is carried on three datasets, and the images are corrupted by AWGN with noise variance level determined by $\{\sigma^2\}$ [40]. Noise is added in the image using the following equation.

$$I_n(x,y) = I_{org}(x,y) + (\frac{1}{\sqrt{2\pi}\sigma})(e^{\frac{-(I_{org}(x,y)-\mu)^2}{2\sigma^2}}). \quad (20)$$

where $I_{org}$ is the original image and $I_n$ is the noisy image. Figure 4 shows the original versus noisy images ($\sigma^2 = \{0.01, 0.02, 0.03\}$) for the three datasets. The second experiment is performed only on the Outex Org. dataset which is corrupted with AWGN noise determined by a self defined noise level discussed in [49].

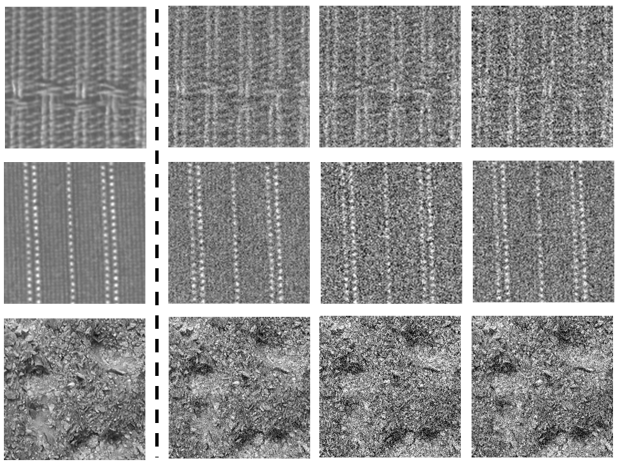


**FIGURE4:** Comparison of original images (leftmost) vs their noisy versions with noise variance $\sigma^2 = \{0.01, 0.02, 0.03\}$ (from left to right).

For a fair comparison, classification accuracy is measured over a fixed number of train and test samples and under a similar classification environment. The datasets and classification environment is discussed in relevant subsections.

This article has been accepted for publication in a future issue of this journal, but has not been fully edited. Content may change prior to final publication. Citation information: DOI 10.1109/ACCESS.2019.2932687, IEEE Access



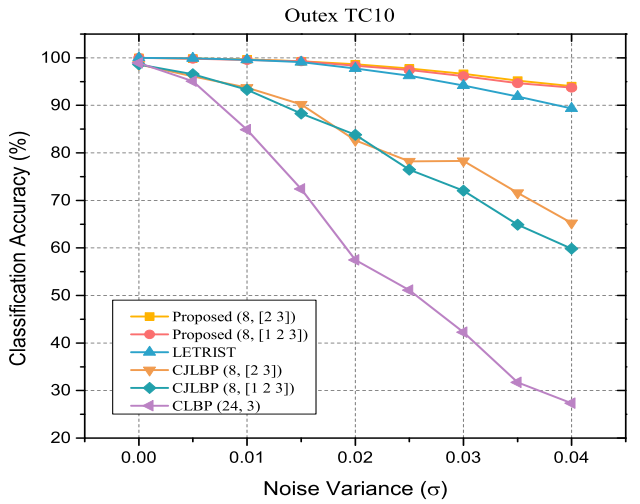


(a)

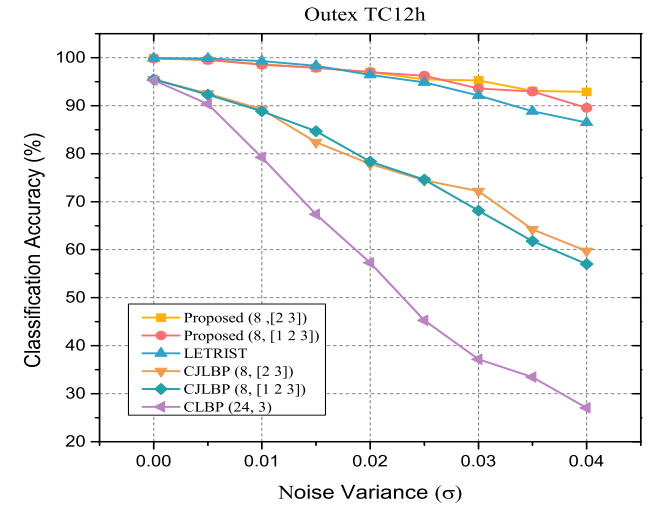


(b)

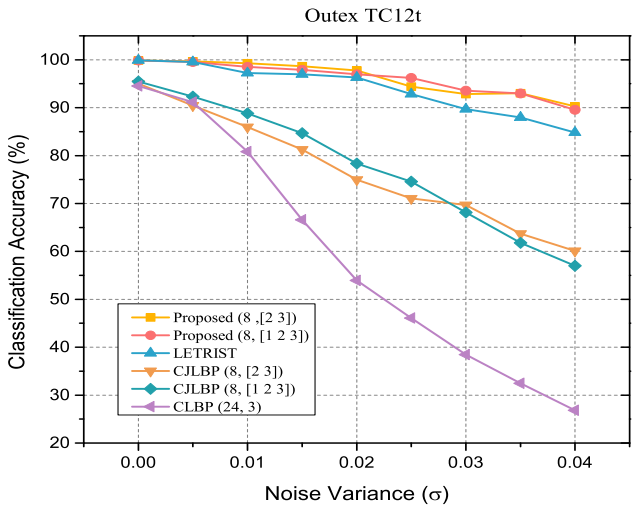


(c)

**FIGURE5:** Classification performance vs noise variance plots of various techniques for Outex Dataset:(a) TC10, (b) TC12h, and (c) TC12t.

### A. OUTEX AND OUTEX EXTENDED

Outex dataset [53] contains images for a variety of image orientations and lightening intensities. The original dataset comprises of twenty-four different texture categories while the extended version contains sixty-eight texture categories and thus provides a more challenging environment compared to the original version. Each category has twenty images of resolution $128 \times 128$. An image is generated for three brightness conditions ("Inca", "TL84" and "Horizon") and for nine different angles of orientation. The following two sub-sets and their extended versions are used:

$Outex\ TC10$: There are $4320\ (24 \times 20 \times 9)$ sample images of inca condition. From these images, $480\ (24 \times 20)$ samples are at an angle of $0°$ and are used as a training set. While the left $3840$ image samples taken under remaining eight angles are used for testing of classification accuracy.

$Outex\ TC12$: It is a bigger collection having $9120\ (24 \times 20 \times 9)$ images. The images have 2 sub-categories, TC12t and TC12h. The $4320$ images for TC12t are captured for illuminate "$T184$" and $4320$ for TC12h are captured under "$horizon"and"TL84$". Training samples are $480\ (24 \times 20)$ images at an angle of $0°$ under illuminate "$inca$".

$Outex\ TC20$: It is an extended version of the TC10 test suite. There are $12,240\ (68 \times 20 \times 9)$ sampled images. $1360$ $(68 \times 20)$ samples are used as a training set. While the left $10880$ image samples are used for testing.

$Outex\ TC24$: It is an extension of TC12 having $4080$ $(68 \times 20 \times 9)$ images. There are two sub-categories, TC24t and TC24h. Training samples are $1360\ (68 \times 20)$ images while $2720\ (68 \times 20 \times 2)$ are used for testing.

### B. KTH-TIPS

The KTH-TIPS (textures under varying illumination, pose and scale) is a challenging material database for texture categorization [54]. It is designed to test the texture operator for varying conditions of lightning, pose, and scale (the distance of material from the camera), unlike CURet dataset, which doesn't provide scale variations [48]. There are ten material categories in total; each class contains eighty-one images. Each material is captured under variable illumination, for nine scale variations and nine poses. We split images of each folder in train and test sets in ratio $(49.4/50.6)$, hence the train set contains $40/81$ random samples and rest are taken for test set [48]. The classification performance is measured as an average of numerical results from a hundred random classification turns.

### C. CLASSIFICATION ENVIRONMENT

A nearest neighbor classifier $(NN\ Classifier)$ is used to classify the extracted feature vectors. Initially, the discriminator is trained with the train feature vectors, for a given dataset and a test feature vector is used to measure the classification performance. The NN classifier classifies the test feature vector based on the Chi-Square statistic. The Chi-Square statistic evaluates dissimilarity between the test

This article has been accepted for publication in a future issue of this journal, but has not been fully edited. Content may change prior to final publication. Citation information: DOI 10.1109/ACCESS.2019.2932687, IEEE Access



**TABLE1:** Classification performance of proposed method vs traditional methods on Outex Org. dataset at $\sigma^2 = 0.025$

| Ref | Method | TC10 | TC12t | TC12h | Average |
|---|---|---|---|---|---|
| [30] | $LBP\ \{T=8, Y=1\}$ | 38.32 | 34.41 | 35.11 | 35.93 |
| [45] | $CLBP\ \{T=8, Y=1\}$ | 35.33 | 31.30 | 33.30 | 33.31 |
| | $CLBP\ \{T=16, Y=2\}$ | 47.71 | 46.04 | 47.10 | 46.41 |
| | $CLBP\ \{T=24, Y=3\}$ | 50.39 | 45.90 | 45.06 | 47.11 |
| [39] | $MRELBP\ \{T=8\}$ | 48.20 | 69.90 | 69.80 | 62.63 |
| [40] | $DALBP\{T=8\}$ | 72.00 | 67.60 | 66.30 | 68.63 |
| [35] | $BRINT\ \{T=8, Y=3\}$ | 73.22 | 68.50 | 67.90 | 69.80 |
| [46] | $CJLBP\_SMC\ \{T=8, Y=(1,2)\}$ | 64.60 | 58.9 | 60.43 | 61.31 |
| | $CJLBP\_S/M/C\ \{T=8, Y=(1,2,3)\}$ | 77.7 | 72.03 | 73.47 | 74.4 |
| | $CJLBP\_SMC\ \{T=8, Y=(2,3)\}$ | 81.60 | 75.60 | 75.57 | 77.59 |
| [47] | $LVQP\_SMC\ \{T=8, Y=1\}$ | 49.30 | 49.50 | 50.00 | 49.6 |
| | $LVQP\_SMC\ \{T=16, Y=2\}$ | 83.00 | 86.00 | 86.80 | 85.20 |
| | $LVQP\_S/M/C\ \{T=24, Y=3\}$ | 91.50 | 87.80 | 87.00 | 88.76 |
| [41] | RINR | 80.70 | - | - | - |
| [43] | $EMCLBP^{eriu246}$ (P, R) = (8, 1) | 91.33 | 85.93 | 88.77 | 88.67 |
| [48] | $LETRIST\ \{L_S=3, L_R=5\}$ | 96.25 | 92.84 | 94.86 | 94.65 |
| **This work** | **RDHD** | **97.76** | **94.39** | **95.42** | **95.86** |

feature vector and all the trained feature vectors. Chi-square statistic is expressed in (21).

$$C(K,L) = \sum_{b=1}^{B} \frac{(K_b - L_b)^2}{(K_b - L_b)}. \tag{21}$$

where $B$ is the total number of bins, $K_b$, $L_b$ are respectively the values of trained and test image at the $b^{th}$ bin. A small value of $C(K,L)$ shows a close similarity between the test vector $K$ and trained vector $L$. The classifier assigns to the test feature vector, the class of train feature vector for which, the Chi-square statistic is small, e.g., the majority of similar class train feature vectors in the nearest neighborhood.

## V. EXPERIMENTAL RESULTS AND ANALYSIS

This section presents the analysis of the noise-robust performance of the proposed hybrid descriptor under a variety of noisy conditions and presents comparisons with closely related descriptors. A variety of parameter settings allows for a comprehensive comparison of the classification performance. The classification accuracy is taken as a measure of feature descriptor's noise sensitivity. When the classification accuracy is high, for a certain variance of the noise, the feature descriptor is said to be noise tolerant. All implementations of the algorithm have been carried out using Matlab 2018a, with core i5, Core 2 Duo 2.6 GHz, 8GB RAM. The comparison of feature dimensionality and computation complexity is presented in Table 2. The results of the two experimental phases are discussed as follows.

**TABLE2:** Feature dimension and computational complexity compared with other methods using an image of size 128 × 128.

| Ref | Descriptor Name | Feature dimension | Feature extraction time (ms) |
|---|---|---|---|
| [37] | VZ-MR8 | 2440 | 262 |
| [38] | BIF | 1296 | 282 |
| [39] | MRELBP | 800 | 293 |
| [35] | BRINT_CSM | 2592 | 246 |
| [45] | CLBP_SMC | 2200 | 119 |
| This Work | **RDHD** | 613 | 224 |

### A. PERFORMANCE ANALYSIS WITH AWGN ($\sigma^2$)

Firstly, we evaluate the performance of the proposed operator for Outex Org. dataset. Fig. 5 presents the performance comparison of proposed descriptor at two parametric conditions (T, Y) e.g., (8, [2, 3]) and (8, [1, 2, 3]) with the techniques CLBP (24, 3), CJLBP (8, [1, 2, 3]), CJLBP (8, [2, 3]) and LETRIST ($L_S$ = 3, $L_R$ = 5). From Fig. 5, it is noticeable that the proposed hybrid operator shows close performance at the given scale-resolution settings. Similar is the case with CJLBP_SMC. Therefore, there is no need to refer to the parameters while discussing the two operators.

We perform analysis by assuming three variance regions: 1) noiseless region where $\sigma^2 = 0$, 2) low noise region, $\sigma^2 \in [0.005\ 0.02]$, and 3) high noise region, $\sigma^2 \in [0.025\ 0.04]$. The following observations can be made:

1) In noiseless region, the hybrid descriptor is comparable to LETRIST achieving an accuracy of $99.9\%$. LETRIST on the other hand performs better than CJLBP_SMC

This article has been accepted for publication in a future issue of this journal, but has not been fully edited. Content may change prior to final publication. Citation information: DOI 10.1109/ACCESS.2019.2932687, IEEE Access



**TABLE3:** Classification performance on outex extended (TC20 and TC24) and KTH-TIPS

| (a) Outex Ext. | Method | Noise Var. $\{\sigma^2\}$ 0 | 0.005 | 0.01 | 0.015 | 0.02 | 0.025 | 0.03 | 0.035 | 0.04 |
|---|---|---|---|---|---|---|---|---|---|---|
| TC20 | $CJLBP\_SMC\ \{T=8, Y=(2,3)\}$ | 90.87 | 37.65 | 34.63 | 33.71 | 32.80 | 32.26 | 31.22 | 30.42 | 11.75 |
| | $LETRIST\ \{L_S=3, L_R=5\}$ | 95.43 | 52.05 | 40.33 | 34.98 | 31.44 | 28.52 | 26.10 | 24.80 | 15.78 |
| | **RDHD** | **95.77** | **58.03** | **46.66** | **40.46** | **35.33** | **32.54** | **30.14** | **28.36** | **17.86** |
| TC24h | $CJLBP\_SMC\ \{T=8, Y=(2,3)\}$ | 82.43 | 37.65 | 34.63 | 33.71 | 32.80 | 32.26 | 31.22 | 30.42 | 11.75 |
| | $LETRIST\ \{L_S=3, L_R=5\}$ | 96.43 | 52.05 | 40.33 | 34.98 | 31.44 | 28.52 | 26.10 | 24.80 | 15.78 |
| | **RDHD** | **96.03** | **58.03** | **46.66** | **40.46** | **35.33** | **32.54** | **30.14** | **28.36** | **17.86** |
| TC24t | $CJLBP\_SMC\ \{T=8, Y=(2,3)\}$ | 82.72 | 37.65 | 34.63 | 33.71 | 32.80 | 32.26 | 31.22 | 30.42 | 11.75 |
| | $LETRIST\ \{L_S=3, L_R=5\}$ | 96.47 | 52.05 | 40.33 | 34.98 | 31.44 | 28.52 | 26.10 | 24.80 | 15.78 |
| | **RDHD** | **96.40** | **58.03** | **46.66** | **40.46** | **35.33** | **32.54** | **30.14** | **28.36** | **17.86** |
| (b) KTH TIPS | | | | | | | | | | |
| | $CJLBP\_SMC\ \{T=8, Y=(3,2)\}$ | 94.63 | 90.75 | 89.00 | 85.73 | 83.08 | 81.66 | 79.49 | 78.34 | 77.59 |
| | $LETRIST\ \{L_S=3, L_R=5\}$ | 98.31 | 96.40 | 94.45 | 92.40 | 91.04 | 87.94 | 85.37 | 83.63 | 81.41 |
| | **RDHD** | **98.26** | **96.14** | **94.14** | **92.87** | **91.22** | **88.74** | **86.52** | **85.90** | **84.13** |

**TABLE4:** Classification performance of proposed method vs traditional methods on Outex Org. dataset at noise level k.

| | | TC10 | | | | TC12h | | | | TC12t | | | |
|---|---|---|---|---|---|---|---|---|---|---|---|---|---|
| Ref | $NoiseParameter$ (k) | 10 | 20 | 30 | 40 | 10 | 20 | 30 | 40 | 10 | 20 | 30 | 40 |
| [45] | $CLBP\ \{T=8, Y=1\}$ | 96.87 | 94.97 | 93.69 | 91.58 | 88.56 | 85.71 | 85.13 | 83.72 | 92.01 | 89.12 | 88.35 | 86.48 |
| | $CLBP\ \{T=16, Y=2\}$ | 98.33 | 97.63 | 96.38 | 93.69 | 94.12 | 91.64 | 90.46 | 87.40 | 95.60 | 93.77 | 91.32 | 89.53 |
| | $CLBP\ \{T=24, Y=3\}$ | 98.80 | 98.12 | 95.62 | 93.33 | 98.80 | 98.12 | 95.62 | 93.33 | 98.80 | 98.12 | 95.62 | 93.33 |
| [49] | $AHP\ \{T=8, Y=1\}$ | 96.40 | 91.50 | 82.10 | 72.1 | 90.00 | 87.50 | 83 | 80 | 89.13 | 85.06 | 82.24 | 79.00 |
| | $AHP\ \{T=16, Y=2\}$ | 99.00 | 98.57 | 96.20 | 90.79 | 95.70 | 94.50 | 92.70 | 87.80 | 94.12 | 92.00 | 90.00 | 87.00 |
| | $AHP\ \{T=24, Y=3\}$ | 99.00 | 98.88 | 96.89 | 89.92 | 96.19 | 94.70 | 92.92 | 89.00 | 97.00 | 95.13 | 90.80 | 89.92 |
| [46] | $CJLBP\_SMC\ \{T=8, Y=(1,2)\}$ | 97.78 | 97.57 | 96.30 | 95.72 | 93.05 | 90.60 | 87.15 | 85.92 | 94.69 | 92.47 | 90.48 | 87.98 |
| | $CJLBP\_SMC\ \{T=8, Y=(1,2,3)\}$ | 98.41 | 98.33 | 97.57 | 96.77 | 94.93 | 93.26 | 91.71 | 89.07 | 96.34 | 94.07 | 92.77 | 91.48 |
| | $CJLBP\_SMC\ \{T=8, Y=(2,3)\}$ | 98.43 | 98.09 | 97.68 | 97.50 | 95.48 | 94.09 | 93.40 | 92.52 | 95.99 | 95.88 | 94.97 | 92.38 |
| | **RDHD** | **100** | **99.95** | **99.79** | **99.71** | **99.72** | **99.35** | **99.26** | **98.13** | **99.93** | **99.75** | **99.54** | **99.21** |

showing high discrimination power. This indicates that LETRIST contributes discriminating features to the proposed operator.

2) In low noise region, the hybrid descriptor shows greater performance than LETRIST with a classification accuracy difference of approximately 1.1% at $\sigma^2 = 0.02$. This indicates that the proposed operator is noise robust than LETRIST and CJLBP_SMC.
3) In high noise region, the hybrid descriptor continues to show high performance. A classification accuracy of 94% at $\sigma^2 = 0.04$ is achieved. This indicates that the proposed operator is able to discriminate texture under high noisy conditions with better accuracy.

To further evaluate the robustness of the proposed operator on Outex dataset, Table 1 presents the comparison with six related techniques over a variety of scale-resolution parameter setting, at noise variance $\sigma^2 = 0.025$. The individual and average classification performance is computed for TC10, TC12h, and TC12t testing suits. The hybrid descriptor is compared to LBP, CLBP, CJLBP, LVQP, BRINT, MRELBP, DALBP, and LETRIST. The operators LVQP and CLBP_SMC are evaluated for the following parametric conditions: (T, Y) $\epsilon$ $\{(8,1),(16,2)$ and $(24,3)\}$, while CJLBP_SMC is evaluated for $(8,[1\ 2]),(8,[1\ 2\ 3])$, and $(8,[2\ 3])$. The best performance of CLBP_SMC is achieved at (24, 3) since the above parameter setting allows to compute both the micro as well as macro-texture. Therefore, the discriminating power of CLBP_SMC is improved. A similar trend in performance is observed for LVQP and CJLBP_SMC. While discussing the results, we will compare the best results of CLBP_SMC, CJLBP_SMC, and LVQP and will avoid mentioning the parameter setting. Noticeably, our method achieves the highest average classification accuracy of 95.86%, indicating that high noise robustness is provided. The operators LBP, CLBP, and MRELBP show degraded performance because the descriptors are not effective in the presence of noise. In comparison to BRINT and DALBP, which show close performance among each other, our descriptor performs with a high margin of approximately 27.23%. The operators LETRIST and LVQP on the other hand, appear as the second and third best performers, respectively.

Table 3 lists the numerical results for Outex Ext. and KTH-TIPS datasets. The performance is evaluated over noise vari-

ance of $\sigma^2 = \{0.005, 0.01, 0.015, 0.02, 0.025, 0.03, 0.035$ and $0.4\}$. The hybrid descriptor is put in comparison with the following two descriptors, CJLBP_SMC [46], and LETRIST [48], with the following parameter setting $\{T = 8, Y = (2, 3)\}$, and $\{L_S = 3, L_R = 5\}$, respectively. For the Outex Ext. dataset following observations can be made. Firstly, the classification accuracy is not close to 90%, indicating the challenging conditions provided by the dataset. Secondly, the trend of performance among the descriptors remains same as in Outex Org. dataset. For example, LETRIST performs better than CJLBP_SMC and the hybrid descriptor outperforms both. This indicates that for the given dataset, the hybrid descriptor also outperforms BRINT, MRELBP and DLABP. In Table 3 (b), a similar trend in performance occurs for KTH-TIPS dataset e.g., proposed $>$ LETRIST $>$ LVQP $>$ CJLBP_SMC. In the light of results of Table 1 and 3 we conclude that the proposed descriptor successfully categorizes the texture in the presence of noise and outperforms the noise robust descriptors e.g., CJLBP_SMC, BRINT, MRELBP, DALBP, LVQP, and LETRIST.

### B. PERFORMANCE ANALYSIS WITH AWGN (K)

Experiment 2 is performed to compare the noise robustness of our proposed descriptor against Adaptive Hybrid Descriptor (AHP) [49] over the range of $k = \{10, 20, 30, 40\}$. Table 4 lists the robustness measure of the proposed descriptor in comparison with CLBP, CJLBP and AHP. The operators AHP and CLBP_SMC are evaluated for the following scale-resolution conditions: (T ,Y) $\epsilon$ $\{(8, 1), (16, 2)$ and $(24, 3)\}$, while CJLBP_SMC is evaluated for $(8, [1\ 2]), (8, [1\ 2\ 3])$ and $(8, [2\ 3])$. From Table 4, it is observed that when k increases for a certain test suit, the classification performance of the texture descriptors decreases. Therefore, the results are discussed only for the worst case of k=40.

From the numerical results, it is observed that AHP achieves the lowest performance. This shows that the methodology adopted by AHP, when compared to the mentioned descriptors, is not effective against noise. CLBP_SMC performs better than AHP, since it involves the usage of global mean magnitude and central gray level. CJLBP_SMC outperforms CLBP_SMC since it involves the operation of multi-scale fusion, which makes it robust against noise. On the other hand, the proposed descriptor outperforms the above descriptors by achieving the highest classification accuracy of 99.71, 98.13, and 99.21 for the respective TC10, TC12h and TC12t test suits at k=40.

From the results of experiment 1 and 2, the performance of the hybrid descriptor on Outex and KTH-TIPS datasets demonstrates that the use of wavelet transform and the proposed feature computation and integration technique offers a robust texture representation.

## VI. CONCLUSION

In this paper, a method of noise robust classification of texture is presented and validated. The proposed method is based on calculating features from low-frequency image information, which forms the basis of our noise robust image model. Three stages are involved in the proposed system. Firstly, multiresolution decomposition of a noisy image is performed, and the low noise components are achieved using 2DDWT. Then, the evaluated components are subjected to LBP based feature extraction. To achieve discrimination power a second feature set is considered, which is based on first and second order differential responses from Gaussian derivative filters. The two feature sets are integrated to obtain a final feature representation that is robust and discriminative in the presence of noise. The hybrid descriptor is examined under a variety of image acquisition conditions provided by following three renowned datasets: Outex original, Outex extended and KTH-TIPS. It is found that the presented descriptor performs robust classification of texture for additive Gaussian noise with varying variance levels of up to $\sigma^2 = 0.04$. The descriptor surpasses other leading techniques such as CJLBP_SMC, BRINT, MRELBP, DALBP, LVQP, AHP, and LETRIST. In future studies, the aim is to reduce the length of the feature vector by considering techniques of feature dimensionality reduction. Moreover, some other methods of noise reduction in an image can be considered to improve the classification performance further.

## REFERENCES

[1] L. Li, C. Jie, F. Paul, Z. Guoying, C. Rama, P. Matti, "A survey of recent advances in texture representation," , vol. 3, 2018, [online] Available: https://urlzs.com/EmPs5.

[2] L. Li, F. Paul, G. Yulan, W. Xiaogang, P. Matti, "Local binary features for texture classification: Taxonomy and experimental study," Pattern Recognit., vol. 62, pp. 135–160, 2017.

[3] Mohan, Arun, Poobal, "Crack detection using image processing: A critical review and analysis", Alex. Eng. J., vol. 57, pp. 787-798, 2018

[4] R. Ruoxu, H. Terence, T. K. Chen, "Automatic Microstructure Defect Detection of Ti-6Al-4V Titanium Alloy by Regions-Based Graph," IEEE Trans. Emerging Topics omputational Intell., vol. 1, no. 2 pp. 87–95, 2017.

[5] F. Reza, S. Ashok, F. Behzad, "Advanced Tissue Characterization and Texture Analysis Using Dual-Energy Computed Tomography Horizons and Emerging Applications," Neuroimaging Clin., vol. 27, pp. 533–546, 2017.

[6] D. Carole, T. Rebecca, S. V., Vineeta, S. Carolina A, B. Hamid, G. Ashish and M. Donna, "Role of quantitative computed tomography texture analysis in the differentiation of primary lung cancer and granulomatous nodules," Quantitative imaging in medicine and surgery, vol. 6, no. 1, pp. 6, 2016.

[7] M. Manoj, V. S. Jochen, M. Robert, A. Hatem, "Texture analysis and machine learning for detecting myocardial infarction in noncontrast low-dose computed tomography: unveiling the invisible," Investig. Radiol., vol. 53, no. 6, pp. 338–343, 2018.

[8] M. Leandro, R. F. Pedro, A. Jefferson, S. J. Wellington, J. A. H. Souza, de Albuquerque, V. Hugo C, "A novel mobile robot localization approach based on classification with rejection option using computer vision," Comput. Electr. Eng., vol. 68, pp. 26–43, 2018.

[9] L. Shan, Y. Wenzhen, A. Edward, C. Anthony G, F. Raul, "Vitac: Feature sharing between vision and tactile sensing for cloth texture recognition," in 2018 IEEE Int. Conf. Robotics and Automation (ICRA), pp. 2722–2727, 2018.

[10] M. Chris, B. James, M. Michael, B. Jonathan, M. Joslin, F. Jennifer, "Automating analysis of vegetation with computer vision: Cover estimates and classification", Ecol. Evol., vol. 8, no. 12, pp. 6005–6015 , 2018.

[11] Y. Yijun, R. Jinchang, L. Yinsheng, W. James FC, I. Winifred, C. Kuo-Ming, "Adaptive fusion of color and spatial features for noise-robust retrieval of colored logo and trademark images," Multidimens. Syst. Signal Process., vol. 27, no. 4, pp. 945–968, 2016.

[12] Y. Yijun, R. Jinchang, L. Yinsheng, W. James FC, I. Winifred, C. Kuo-Ming, "Adaptive fusion of color and spatial features for noise-robust

retrieval of colored logo and trademark images," Multidimens. Syst. Signal Process., vol. 27, no. 4, pp. 945–968, 2016.

[13] F. Elias, P. George, G. Maria, F. George, "An automatic target detection algorithm for swath sonar backscatter imagery, using image texture and independent component analysis," Remote Sens., vol. 8, no. 5, pp. 373, 2016.

[14] Deshmukh, Gaurav V., B. Smriti H, "Facial Expression Recognition using Bandlet Transform and Centre Symmetric-Local Binary Pattern" in 2018 5th Int. Conf. Signal Process. Integr. Netw. (SPIN), pp.726–729, 2018.

[15] Z. Yuqian, L. Ding, H. Thomas, "Survey of Face Detection on Low-quality Images," in 2018 13th IEEE Int. Conf. Automatic Face Gesture Recognit. (FG 2018), pp. 769–773, 2018.

[16] Athira. AP, V. Midhula, Mohan. R., "Moving Object Detection Using Local Binary Pattern and Gaussian Background Model," Ind. Interact. Innov. Sci., Eng. Tech., vol. 1, pp. 367–376 ,2018

[17] K. Shiva, S. Reza, "Vehicle detection, counting and classification in various conditions," IET Intell. Transp. Syst., vol. 10, no. 6, pp. 406–413, 2016.

[18] L. Jinzhu, Z. Dong, J. Huanyu, "Discriminating Leaves Affected with Tomato Yellow Leaf Curl through Fluorescence Imaging Using Texture and Leaf Vein Features," Transact. ASABE, vol. 59, no. 6, pp.1507–1515, 2016.

[19] L. Patrick, E. Robin, S.Natalie NC, G. Sanjay, F. Michael, M. Anant, "Stable and discriminating features are predictive of cancer presence and Gleason grade in radical prostatectomy specimens: a multi-site study," Scientific reports, vol. 8, no. 1, pp. 14918, 2018.

[20] Y. Guo, G. Zhao, and M. PietikaInen, "Discriminative features for texture description," Pattern Recognit., vol. 45, no. 10, pp. 3834–3843, Oct. 2012

[21] L. Liheng, L. Yuhui, X. Liang, Li. Zhenjiang, L. Han, D. Ningning, L. Wenwu, Y. Zhenghan, W. Zhenchang, J. Erhu, "Application of texture analysis based on apparent diffusion coefficient maps in discriminating different stages of rectal cancer," J. Magn. Reson. Imaging, vol. 45, no. 6, pp. 1798–1808, 2017.

[22] Y. Peng, Z. Fanlong, Y. Guowei, 'Fusing DTCWT and LBP based features for rotation, illumination and scale invariant texture classification," IEEE access, vol. 6, pp. 13336–13349, 2018.

[23] D. Chathurika, M. Sasan, B. Michael, N. Mahesan, "Rotation invariant texture descriptors based on Gaussian Markov random fields for classification," Pattern Recognit. Lett., vol. 69, pp. 15–21, 2016.

[24] Z. Lefei, Z. Qian, D. Bo, H. Xin, T. Y. Yan, T. Dacheng, "Simultaneous spectral-spatial feature selection and extraction for hyperspectral images," IEEE Transact. Cybern., vol. 48, no. 1, pp. 16–28, 2018.

[25] X. Hong, G. Zhao, M. Pietikainen, and X. Chen, "Combining LBP difference and feature correlation for texture description," IEEE Trans. Image Process., vol. 23, no. 6, pp. 2557–2568, Jun. 2014.

[26] A.Ömer F et al., "Multi-category EEG signal classification developing time-frequency texture features based Fisher Vector encoding method," Neurocomputing, vol. 218, pp. 251–258, 2016.

[27] R. C. Gonzalez, "Image Restoration and Reconstruction", Digital Image Process, 3rd ed., India: Pearson Prentice Hall, 2011, 322-330

[28] D. Steven, S. Vincent, B. Stephen, W. Gordon, H. Felix, "Dirty pixels: Optimizing image classification architectures for raw sensor data,", 2017, [online] Available: https://arxiv.org/abs/1701.06487

[29] S. Zhun, O. Mete, Z. Yan, L. Xing, O. Takayuki, "Feature quantization for defending against distortion of images, in " Proc. IEEE Conf. Comput. Vis. Pattern Recognit., pp. 7957–7966, 2018.

[30] T. Ojala, M. Pietikainen, T. Maenpaa, "Gray scale and rotation invariant texture classification with local binary patterns," Eur. Conf. Comput. Vision, pp. 404–420, 2000

[31] X. Tan, B. Triggs, "Enhanced local texture feature sets for face recognition under difficult lighting conditions," IEEE Trans. image Process., vol. 19, pp. 1635–1650, 2010.

[32] T. Ahonen, M. Pietikainen, "Soft histograms for local binary patterns," in Proc. Finnish Signal Process. Symp., FINSIG, vol. 5, no. 9, pp. 1, 2007.

[33] J. Ren, X. Jiang, J. Yuan, " Noise-resistant local binary pattern with an embedded error-correction mechanism," IEEE Trans. image Process., vol. 22, pp. 4049-4060, 2013.

[34] J. Chen, V. Kellokumpu, G. Zhao, M. Pietikainen, "RLBP: Robust Local Binary Pattern," BMVC, vol. 106, pp. 68-76, 2013.

[35] L. Liu, Y. Long, P. W. Fieguth, S. Lao, G. Zhao, "BRINT: binary rotation invariant and noise tolerant texture classification," IEEE Trans. image Process., vol. 23 ,pp. 3071-3084, , 2014.

[36] T. Song, H. Li, F. Meng, Q. Wu, B. Lua, B. Zeng, M. Gabbouj , "Noise-robust texture description using local contrast patterns via global measures," IEEE signal Process. Lett., vol. 1 , pp. 93–96, 2014.

[37] M. Varma and A. Zisserman, "A statistical approach to texture classification from single images," Int. J. Comput. Vision., vol. 62, no. 1, pp. 61âĂŞ81, 2005.

[38] M.Crosier, and L. D. Griffin, "Using basic image features for texture classification," International journal of computer vision., vol.88, no. 3, pp. 447-460, 2010.

[39] L. Liu, S. Lao, P. W. Fieguth, Y. Gua, X. Wang, M. Pietikainen, "Median robust extended local binary pattern for texture classification," IEEE Int. Conf. image Process. (ICIP), vol. 25, 2015.

[40] Z. Pan, X. Wu, Z. Li, Z. Zhou, "Local adaptive binary patterns using diamond sampling structure for texture classification," IEEE signal Process. Lett., vol. 24 ,pp. 828–832, 2017.

[41] M. M. Feraidooni, and D. Gharavian, "A new approach for rotation-invariant and noise-resistant texture analysis and classification," Machine Vision and Applications., vol. 29, no. 3, pp. 455-466, 2018.

[42] H. Hadizadeh, "Multi-resolution local Gabor wavelets binary patterns for gray-scale texture description," Pattern Recognition Letters., vol. 65, pp. 163-169, 2015.

[43] M. H. Shakoor, and R. Boostani, "Extended mapping local binary pattern operator for texture classification," International Journal of Pattern Recognition and Artificial Intelligence., vol. 31, no. 06, pp. 1750019, 2017.

[44] Fawad, M. J. Khan, M. A. Riaz, H. Shahid, M. S. Khan, Y. Amin, J. Loo, and H. Tenhunen "Texture Representation through Overlapped Multi-oriented Tri-scale Local Binary Pattern", IEEE Access, vol. 7, no. 1, pp. 66668-66679, May. 2019.

[45] Z. Guo, L. Zhang, D. Zhang, "A completed modeling of local binary pattern operator for texture classification," IEEE Trans. image Process., vol. 19, pp. 1657–1663, 2010.

[46] X. Wu, J. Sun, "Joint-scale LBP: a new feature descriptor for texture classification," Vis. Comput., vol. 33 ,pp. 317–329, 2017.

[47] P. Zhibin, F. Hongcheng, Z. Li, "Texture classification using local pattern based on vector quantization," IEEE Trans. image Process., vol. 24, no. 12, pp. 5379–5388, 2015.

[48] T. Song, H. Li, F. Meng, Q. Wu, J. Cai, "Letrist: locally encoded transform feature histogram for rotation-invariant texture classification," IEEE Trans. circuits Syst. video Tech., vol. 28 no. 7, pp. 1565–1579, Jul. 2018

[49] Z. Ziqi, Y. Xinge, C. C. Philip, T. Dacheng, O. Weihua, J. Xiubao, Z. Jixin, "An adaptive hybrid pattern for noise-robust texture analysis," Pattern Recognit., vol. 48, no. 8, pp. 2592–2608, 2015.

[50] J. R. Benjamin, and T. Jayasree, "Improved medical image fusion based on cascaded PCA and shift invariant wavelet transforms," International journal of computer assisted radiology and surgery., vol. 13, no. 2, pp. 229-240, 2018.

[51] B. Adel, J. Abdolabbas, N. S. Mehdi, Z. Dariush, "Weed segmentation using texture features extracted from wavelet sub-images," Biosyst. Eng., vol. 157, pp. 1–12, 2017.

[52] B. Adel, J. Abdolabbas, N. S. Mehdi, Z. Dariush, "Mammogram classification using two dimensional discrete wavelet transform and gray-level co-occurrence matrix for detection of breast cancer," Neurocomputing, vol. 154, pp. 1–14, 2015.

[53] T. Ojala, T. Maenpaa, M. Pietikainen, J. Viertola, J. Kyllonen, S. Huovine, "Outex - new framework for empirical evaluation of texture analysis algorithms," Object Recogniion. supported by user interaction for service robots, vol. 1, pp. 701–706, 2002.

[54] M. Fritz, E. Hayman, B. Caputo, J. O. Eklundh, "On the significance of real-world conditions for material classification," in Eur. Conf. Comput. vision (ECCV), pp. 253–266, 2004.

This article has been accepted for publication in a future issue of this journal, but has not been fully edited. Content may change prior to final publication. Citation information: DOI 10.1109/ACCESS.2019.2932687, IEEE Access



AYESHA received her B.Sc. degree in Telecommunication from University of Engineering and Technology Taxila, Pakistan, in 2017. She joined Association for Computing Machinery (ACM) society in 2016 and played active part as finance secretary and general member. She has actively organized many technical events in university campus. She is currently pursuing the M.Sc. thesis in Telecommunication Engineering from the same university. Her research interests include information security systems, computer vision, pattern recognition, and image processing.

FAWAD received his BS degree in Telecommunication from National University of Modern Languages, Pakistan, in 2011. In 2012, he joined Zong China mobile company as Transmission Engineer. He received MS degree from the Military College of Signals, National University of Science and Technology, Pakistan in 2016, which was followed by his Graduate Assistant job in Ghulam Ishaq Khan Institute of Engineering Sciences and Technology. He is currently pursuing the Ph.D. thesis in Telecommunication Engineering from University of Engineering and Technology Taxila, Pakistan. His research interests include computer vision, pattern recognition, and image processing.

MUHAMMAD JAMIL KHAN received the B.Sc. Engineering degree in Computer Engineering, The M.Sc. degree in Telecommunication Engineering, and the Ph.D. degree in Computer Engineering from University of Engineering and Technology, Taxila, Pakistan, in 2005, 2009 and 2016 respectively. He is currently Assistant Professor and director of Embedded Systems and Digital Signal Processing Laboratory in the same University. He is also the founder of Virtual Reality Simulation Laboratory at the University. He has authored or co-authored numerous technical articles in well-known international journals and conferences. His current research interests include multimedia content analysis, RF identification and machine learning.

MUHAMMAD ALI RIAZ received his M.S. and B.S. degree in Electrical Engineering from Iowa State University, USA in 2010 and 2009 respectively. Afterwards, he joined the Department of Electrical and Computer Engineering, Iowa State University, USA as a Research Assistant. He is currently serving as Assistant Professor associated with ACTSENA research group at University of Engineering and Technology, Taxila. Ali is working towards the design and implementation of chipless RFID tags based on electromagnetic signature and their signal processing applications. He also serves as the director of Electronics and Measurements laboratory at his department. His research work has been featured in a number of ISI-indexed journals.

HUMAYUN SHAHID received his BS degree in Communication Systems Engineering from the Institute of Space Technology, Islamabad in 2008. He joined Space and Upper Atmosphere Research Commission (SUPARCO) where he worked on radiation-hardened space grade components for telemetry subsystems. In 2011, Humayun completed his MS in Signal Processing from Nanyang Technological University, Singapore. Thereafter, he joined the department of telecommunication engineering at the University of Engineering and Technology, Taxila where he currently works as an Assistant Professor. Humayun is affiliated with the ACTSENA research group working towards design and signal processing-related aspects of electromagnetic transduction-based sensor-incorporated chipless RFID tags. He is also the director at the departmental Antenna and RF laboratory. His research work has been featured in a number of ISI-indexed journals and international conferences.

MANSOOR SHAUKAT KHAN received his B.Sc. degree from PU Lahore, Pakistan in 1994, M.Sc. degrees in Statistics from University of ARID Agriculture Rawalpindi, Pakistan in 2000. He received his Ph.D. from Beijing Institute of Technology (BIT), P.R. China in January 2016. Currently, he is working as an Assistant Professor, department of mathematics, at COMSATS University Islamabad, Pakistan. His research interests include mathematical modeling & optimization, quality & reliability engineering, survival analysis, spatial data analysis, and data science. He has more than 10 research papers in reputed journals and proceedings of international conferences. Most recently he received National Research Program for Universities award from HEC Pakistan.

YASAR AMIN received the BSc degree in Electrical Engineering with specialization in Telecommunication and MBA in Innovation and Growth from Turku School of Economics, University of Turku, Finland. His MSc is in Electrical Engineering with specialization in System on Chip Design, and also Ph.D. is in Electronic and Computer Systems from Royal Institute of Technology (KTH), Sweden, with the research focus on printable green RFID antennas for embedded sensors. He is currently an Associate professor and chairman of Telecommunication Engineering Department, University of Engineering and Technology Taxila, Pakistan. He also serves as the Director of Embedded Systems Research and Development Centre. He is the founder of ACTSENA (Agile Creative Technologies for Smart Electromagnetic Novel Applications) research group. He has authored or co-authored more than 100 international technical papers in conferences and journals. His research interests include the design and application of multiple antenna systems for next generation mobile communication systems, millimeter-wave and terahertz antenna array, implantable & wearable electronics, and inkjet printing technology in microwave applications. He is a member of more than a dozen international professional societies and the fellow of PAE.

JONATHAN LOO received his MSc degree in Electronics from the University of Hertfordshire, UK in 1998 and his Ph.D. degree in Electronics and Communications from the same university in 2003. He leads a research team of 8 Ph.D. students in the area of communication and networking. He is presently Professor and Chair in Computing and Communication Engineering in School of Computing and Engineering University of West London, UK. His research interest includes network architecture, communication protocols, network security, embedded systems, video coding and transmission, wireless communications, digital signal processing, and optical networks. He has successfully graduated 13 PhDs as Principle Supervisor and contributed over 175 publications in the aforementioned specialist areas.

HANNU TENHUNEN is Chair Professor of Electronic Systems at Royal Institute of Technology (KTH), Stockholm, Sweden. He has been full professor, invited professor or visiting honorary professor in Finland (TUT, UTU), Sweden (KTH), USA (Cornel U), France (INPG), China (Fudan and Beijing Jiaotong Universities), and Hong Kong (Chinese University of Hong Kong), and has an honorary doctorate from Tallinn Technical University. He has been the director of multiple national large-scale research programs or being an initiator and director of national or European graduate schools. He has actively contributed to VLSI and SoC design in Finland and Sweden via creating new educational programs and research directions, most lately at European level as being the EU-level Education Director of the new European flagship initiative European Institute of Technology and Innovations (EIT), and its Knowledge and Innovation Community EIT ICT Labs. He is the founding editorial board member of 3 scientific journals and guest editor for multiple special issues of scientific journals and books. He has authored or co-authored more than 900 international technical papers in conferences and journals. He has been granted 9 foreign patents he is a member of Academy of Engineering Science of Finland.